HHS Public Access

Author manuscript

Brain Topogr. Author manuscript; available in PMC 2019 November 01.

Published in final edited form as:

Brain Topogr. 2018 November ; 31(6): 985–1000. doi:10.1007/s10548-018-0664-5.

Response hand and motor set differentially modulate the connectivity of brain pathways during simple uni-manual motor behavior

Alexandra Morris[1], **Mathura Ravishankar**[1], **Lena Pivetta**[1], **Asadur Chowdury**[1], **Dimitri Falco**[2], **Jessica S. Damoiseaux**[3,4], **David R. Rosenberg**[1], **Steven L. Bressler**[2], and **Vaibhav A. Diwadkar**[1]

[1]Dept. of Psychiatry & Behavioral Neurosciences, Wayne State University School of Medicine

[2]Center for Complex Systems and Brain Sciences, Florida Atlantic University

[3]Dept. of Psychology, Wayne State University

[4]institute of Gerontology, Wayne State University

Abstract

We investigated the flexible modulation of undirected functional connectivity (uFC) of brain pathways during simple uni-manual responding. Two questions were central to our interests: 1) Does response hand (dominant vs. non-dominant) differentially modulate connectivity and 2) are these effects related to responding under varying motor sets. fMRI data were acquired in twenty right-handed volunteers who responded with their right (dominant) or left (non-dominant) hand (blocked across acquisitions). Within acquisitions, the task oscillated between periodic responses (promoting the emergence of motor sets) or randomly induced responses (disrupting the emergence of motor sets). Conjunction analyses revealed eight shared nodes across response hand and condition, time series from which were analyzed. For *right hand* responses connectivity of the M1 ⟷ Thalamus and SMA ⟷ Parietal pathways was more significantly modulated during *periodic* responding. By comparison, for *left hand* responses, connectivity between five network pairs (including M1 and SMA, insula, basal ganglia, premotor cortex, parietal cortex, thalamus) was more significantly modulated during *random* responding. uFC analyses were complemented by directed FC based on multivariate autoregressive models of times series from the nodes. These results were complementary and highlighted significant modulation of dFC for SMA → Thalamus, SMA → M1, basal ganglia → Insula and basal ganglia → Thalamus. The results demonstrate complex effects of motor organization and task demand and response hand on different connectivity classes of fMRI data. The brain's sub-networks are flexibly modulated by factors related to motor organization and/or task demand, and our results have implications for assessment of medical conditions associated with motor dysfunction.

Address Correspondence to: Vaibhav A. Diwadkar, PhD, Professor, Brain Imaging Research Division, Department of Psychiatry and Behavioral Neuroscience, Wayne State University School of Medicine, Suite 5A, Tolan Park Medical Building, 3901 Chrysler Service Drive, Detroit, MI 48201 USA, vdiwadka@med.wayne.edu Ph: +1.313.577.0164 Fax: +1.313.577.5900.

Keywords

Uni-manual responses; Motor organization; Right-Handers; fMRI; Functional connectivity; Granger causality

Introduction

Sensori-motor systems are among the most exquisitely organized within the brain's functional networks. fMRI studies reveal "hard-wired" properties such as *handedness* (Amunts et al., 1996; Tzourio-Mazoyer et al., 2015), but also show that regional and inter-regional responses can be responsive to task-induced modulation. The trait-related representations of handedness interact in predictable (and unpredictable) ways with variations in motor task demand (Witt & Stevens, 2013). For instance, during rapid visual detection tasks (when stimuli are briefly presented to one visual hemi-field, and therefore one visual cortex) fMRI activation profiles are modulated by the response hand used to signal a response. When right handed individuals respond with their dominant hand, more extensive activation profiles are observed particularly when the stimulated visual cortex is contra-lateral to the responding (left) motor cortex (that is under more demanding conditions)(Diwadkar, Bellani, et al., 2017). Separately, network interactions between regions such as the dorsal anterior cingulate cortex (dACC) and the supplementary motor cortex (SMA) are differentially modulated during basic visuo-motor integration tasks that demand motor responses to periodic or non-periodic presentations of visual stimuli (Asemi, Ramaseshan, Burgess, Diwadkar, & Bressler, 2015; Diwadkar, Asemi, Burgess, Chowdury, & Bressler, 2017; Friedman et al., 2017). Thus, network interactions induced by motor tasks can be representative of both the motor organization of the cortex (Grefkes, Eickhoff, Nowak, Dafotakis, & Fink, 2008), and the functional modulation of this organization by task (Goble et al., 2010; Hoffstaedter et al., 2014; Paus, 2001). Understanding how response hand *and* basic motor demands individually or interactively modulate brain network activation has implications for the characterization of both neurodegenerative (Nuber et al., 2008) and neuropsychiatric disorders (Abboud, Noronha, & Diwadkar, 2017; Friedman et al., 2017). Many of these disorders are associated with misrepresentations of effectors in the motor cortex and/or dysregulation of basic mechanisms of motor control. For example, prior work demonstrates brain network dysfunction in patients with obsessive compulsive disorder after performing a simple uni-manual motor task both using fMRI (Friedman, et. al., 2017) as in the present study and with other neuroimaging tools such as EEG (Velikova, et. al., 2010). In this study, we deployed a simple uni-manual response paradigm created by manipulating the periodicity of a presented visual probe to drive basic finger movements (Asemi et al., 2015; Diwadkar, Asemi, et al., 2017). Varying periodicity provides a simple framework for manipulating the demands of visuo- motor integration, either promoting the use of a motor set (periodic presentation of the probe) or disrupting the reliance on such a set (pseudo random presentation). Here we focused on network characterizations of the core and extended motor network, by modeling interactions using a) undirected functional connectivity (uFC) models (Friston, 2011; Silverstein, Bressler, & Diwadkar, 2016) well suited for the flexible assessment of bi-directional changes in the brain's functional connectome; b) uFC analyses were complemented using a class of Granger Causality

models (Bressler & Seth, 2011; Bressler, Tang, Sylvester, Shulman, & Corbetta, 2008), based on multi-variate autoregressive models (Asemi et al., 2015; Diwadkar, Asemi, et al., 2017). MVAR models are well optimized for assessing asymmetric directed interactions between nodes estimated from time series data, using a more complex statistical framework for network discovery between network pairs (Silverstein et al., 2016).

In the study (restricted to right handed participants), we modeled the effects of the factorial combination of response hand (dominant vs. non-dominant) and task demand (where the onsets of stimuli were periodic or random). For dFC analyses, directional effects ($A \rightarrow B \neq B \rightarrow A$) were modeled as an additional factor.

A rationale for the evaluated motor network

Well circumscribed tasks can be used as cognitive scalpels that systematically modulate brain activity (Goense & Logothetis, 2008), because brain regions are flexibly recruited in the service of tasks (Park & Friston, 2013). Thus, data aggregation and meta-analyses provide a powerful framework for reliably identifying brain regions activated in specific domains (Eickhoff, Bzdok, Laird, Kurth, & Fox, 2012), and applied to motor function has resulted in the identifying regions that constitute core and extended areas of the brain's motor networks (Witt, Laird, & Meyerand, 2008). The primary motor cortex (M1), specifically on the mid-lateral aspect, is essential in performing discrete forefinger muscle movements and it is known that the contralateral motor cortex directs these movements, due to the crossing of the cortico-spinal tract (Lotze et al., 2000; Sarfeld et al., 2012; Volkmann, Schnitzler, Witte, & Freund, 1998). The supplementary motor area (SMA) is important for the planning and initiation of movement and its engagement is indicated in proactive-type motor tasks (Asemi et al., 2015; Grafton, Hazeltine, & Ivry, 2002; Grafton, Mazziotta, Woods, & Phelps, 1992). Both regions evince a high degree of connectivity with thalamic nuclei providing a pathway through which sensory inputs can directly innervate the core motor system (Guye et al., 2003). Other sub-cortical regions are also critical in the cortical - subcortical interplay that sub serves motor function. The basal ganglia are implicated in the synchronicity of motor movements and coupling signals across brain networks (Lehericy et al., 2006). There is substantial functional heterogeneity of the insular cortex, with the structure associated with autonomous and non-cognitive functions such as interoception and thermoregulation (Diwadkar, Murphy, & Freedman, 2014; Muzik & Diwadkar, 2016), but also higher order cognitive functions including attention, emotion and salience processing (Uddin, Nomi, Hebert-Seropian, Ghaziri, & Boucher, 2017); Its role in motor function may be sub served by aspects of if its structural connectivity to motor control regions such as the dorsal anterior cingulate cortex (Ghaziri et al., 2017). The parietal lobe is central to visual sensory integration (Fogassi et al., 2005; Fogassi & Luppino, 2005), a task element that is central to the employed paradigm (Friedman et al., 2017). Frontal regions including the premotor cortex (PMC) and (as suggested earlier), the dorsal anterior cingulate cortex (dACC) become engaged during motor tasks: This engagement is respectively thought to be associated with the initiation of finger movements (Cunnington, Windischberger, Deecke, & Moser, 2003), and mechanisms of motor control (Asemi et al., 2015; Diwadkar, Asemi, et al., 2017; Paus, 2001).

Hemispheric organization is a central organizing principle for the brain's motor system (Kim et al., 1993), and approximately 90% of the adult population is right handed. The neurobiological bases of right handedness have been known from classic studies in neurology. Liepmann (Liepmann, 1905) showed that left hemispheric lesions more often result in apraxia than right hemispheric lesions, suggestive of an asymmetric motor control system. Recent experimental work continues to the illuminate functional expressions of this asymmetry. For example, simple motor movements evoke highly asymmetric patterns of effective connectivity in right handed participants, and the degree of this asymmetry is greater than what is observed in left handers (Pool, Rehme, Fink, Eickhoff, & Grefkes, 2014). These effects converge with diffusion tensor imaging data showing that right handers are characterized by increased asymmetry in structural connectivity (Seizeur et al., 2014). And, as previously noted, dominant right handed responses during inter-hemispheric visual integration tasks evince activations that are asymmetric relative to left handed responses in the same participants (Diwadkar, Bellani, et al., 2017).

Motor control is a central element underlying the motor system, and is likely to interact with handedness and response hand. There is limited prior work that has systematically assessed how motor network connectivity is modulated by response hand (dominant vs. non-dominant) under parametrically varied task conditions even though extent evidence indicates highly asymmetric and favored (toward right handers) patterns of intrinsic functional connectivity (Pool, Rehme, Eickhoff, Fink, & Grefkes, 2015). Therefore, here we examined how both the undirected and directed functional connectivity of sub-networks within the previously described network of regions was differentially modulated when right handed participants responded with their right or left hand. The visuo-motor integration task used was characterized by varying demands on control, resulting from a simple manipulation of the periodicity of the demanded motor response (Friedman et al., 2017). In effect, the overall experimental design employed a factorial combination of response hand (Right/Dominant vs. Left/Non-Dominant) and task condition (Random vs. Periodic).

Materials and Methods

Participants

Twenty participants (Age Range: 17–22 yrs., Mean = 19 yrs.; 10 females) provided informed consent for the fMRI study. The study received ethics approval from the institutional review board at the Wayne State University School of Medicine and participants received monetary compensation for their participation. Right-handedness in all participants was established using the structured Neurological Evaluation Scale (Buchanan & Heinrichs, 1989), and all participants were evaluated for, and ensured to be free of psychiatric and neurological conditions (First, Gibbon, Spitzer, Williams, & Benjamin, 1997).

Task

The basic visuo-motor integration paradigm has been independently employed in previous work to study basic motor control mechanisms (Asemi et al., 2015; Diwadkar, Asemi, et al., 2017; Friedman et al., 2017). The paradigm involves the repeated presentation of a white visual stimulus (RGB: 255, 255, 255; extent: 34 × 32 mm; subtended visual angle: ~17^{o};

Stimulus duration: 100 ms), at the center of a display panel. Participants were instructed to tap with the forefinger of their responding hand (Dominant: Right or Non-Dominant Left) in response to its presentation. The inter-stimulus interval (ISI) was varied across conditions. Thus, to effectively induce (potentially differential) fMRI estimated neuronal responses, the periodicity of the stimulus was varied by task epoch: During *Periodic* epochs, the inter-stimulus interval (ISI) between successively presented stimuli was fixed, whereas during *Random* epochs, the ISI was jittered. To maintain a comparable number of elicited responses across Periodic and Random epochs, the ISIs for the random periods were created by randomly sampling values from Gaussian distributions ($\mu = 1.0$ s and $\sigma = 0.5$ s or $\mu = 2.0$ sand $\sigma = 1.0$ s; the lower bound on ISI was 300 ms). Thus, the ISI during Random epochs were adjusted to ensure that the number of elicited responses was equal to the Periodic counterpart. All finger responses were collected from the receptive surface (extent: 33 * 33 mm) of a fiber-optic response touchpad (Current Design Systems, Inc.) interfaced with the Presentation software package (Neurobehavioral Systems, Inc.).

Response hand was blocked across scans; participants responded only with the Right *or* Left hand during each of the two fMRI acquisitions (order counterbalanced across participants). Within each of the two scans, four Periodic and four Random epochs (30 s each) were employed, in addition to interspersed rest epochs (20 s). During the rest condition, participants were instructed to fixate on a cross hair in the center of the display panel.

fMRI Collection

Gradient echo EPI fMRI data acquisition was conducted at the Vaitkevicius Magnetic Resonance Centre on a 3T Siemens Verio system using a 12-channel volume head coil (TR: 2.6s, TE: 29ms, FOV: 256×256mm^2, acquisition matrix: 64×64, 36 axial slices, voxel dimensions: 3.75 × 3.75 × 3 mm^3). In addition, a 3D T1-weighted anatomical MRI image was acquired (TR: 2200ms, TI: 778ms, TE: 3ms, flip-angle=13°, FOV: 256×256mm2, 256 axial slices of thickness = 1.0mm, matrix=256×256). A neuroradiologist reviewed all scans to rule out clinically significant abnormalities. Each of the two fMRI acquisitions lasted approximately 6 min and 30 s.

Image Preprocessing

MR images were preprocessed and analyzed using SPM 8 (Statistical Parametric Mapping, Wellcome Department of Imaging and Neuroscience, London, UK) using established methods for temporal (slice timing correction) followed by spatial preprocessing. For spatial pre-processing, the EPI images for each of the scans were manually oriented to the AC-PC line with the reorientation vector applied across the EPI image set, realigned to a reference image to correct for head movement, and coregistered to the anatomical high resolution T_1 image. This high-resolution T_1 image was normalized to the MNI template, with the resultant deformations subsequently applied to the co-registered EPI images for normalization. Low frequency components were removed using a low-pass filter (128 s) and images were spatially smoothed using a Gaussian filter (8 mm full-width half maximum; FWHM). An autoregressive AR (1) model was used to account for serial correlation, and regressors modeled as boxcar vectors (for each of the task-related conditions: Periodic, Random and Rest) were convolved with a canonical hemodynamic reference waveform,

with the six motion parameters included as effects of no interest. For each of the 20 subjects, two activation maps for each response hand (one for each of the task conditions) was forwarded for second level analyses. Thus, each subject contributed four sets of activation profiles.

Second-level (group) activation analyses were performed using a random effects within-subject's two-way analysis of variance with the two experimental factors (Response Hand and Periodicity) as the principal independent variables of interest. The goal of these preliminary analyses was to harvest seeds, the time series from which would be forwarded for uFC analyses. From the second level random-effects model, a conjunction analysis using the minimum inference statistic was performed to identify a common substrate of regions activated across *both* response hands (Nichols, Brett, Andersson, Wager, & Poline, 2005). Significant clusters in regions of interest were identified using 10^4 Monte Carlo simulations of the data to identified minimum cluster extents ($p<0.05$, cluster-level) (Ward, 2000) by estimating the minimum cluster extent in order for activated clusters to be rejected as false positive (noise-only) clusters. The Monte Carlo alpha probability simulation computes the probability of a random field of noise (after accounting for spatial correlations of voxels based on the image smoothness within each region of interest estimated directly from the data set). The resultant cluster size reflects a minimum cluster extent, after thresholding the noise at a given level. Thus, instead of using only the individual voxel probability threshold in achieving the desired overall significance level, the method uses a combination of both probability thresholding and minimum cluster size thresholding. The underlying assumption is that true regions of activation will occur over contiguous voxels whereas noise has much less of a tendency to form clusters of activated voxels.

The conjunction analyses identified seven nodes of interest for subsequent uFC and dFC analysis, and the peak locations were labeled using deterministic stereotactic atlases (Maldjian, Laurienti, Kraft, & Burdette, 2003). The network of nodes is depicted in Figure 1 (see Table 1 for statistical information).

Undirected Functional Connectivity (uFC) Analysis

uFC analysis was performed using previously published methods (Whitfield-Gabrieli & Nieto-Castanon, 2012), and the seven nodes of interest identified using conjunction analyses were forwarded for analyses. Across the sample, two analytic sessions were created, one for each hand. Segmentation of structural (T_1) images was performed and the resulting Grey Matter and Cerebrospinal Fluid (CSF) images were co-registered with the functional (T_2) scans. The BOLD signals from white matter and CSF masks, and the motion regressors were set as confounds, using the default orthogonal time series estimated principal component analysis (PCA). The temporal confounding factors were then regressed from the BOLD time series at each voxel and the residual time series are band pass filtered (0.01 Hz - 0.1Hz) to eliminate low frequency drifts. ROI time series were extracted by averaging across all the voxels within each individual ROI. uFC between two regions was computed using a zero-lagged bivariate-correlation, estimating the linear association between two BOLD signals. Two factors, the response hand used during the acquisition (right vs. left), and the task condition (random vs. periodic) were modeled as the factors of interest. The task related

effects for each condition were determined at the group level using the beta value, *t* statistic (two-sided *t* test), and false discovery rate (FDR) corrected *p* values.

Directed Functional Connectivity (dFC) Analysis

Directed functional connectivity (dFC) was estimated using MultiVariate AutoRegressive (MVAR) models. The MVAR model is a statistical framework for estimating the strength of the directional effects between nodal pairs (A, B: A → B, B → A), with the model coefficient encoding the magnitude of this strength (Asemi et al., 2015; Bressler & Seth, 2011; Diwadkar, Asemi, et al., 2017; Tang, Bressler, Sylvester, Shulman, & Corbetta, 2012). This strength serves as a metric of the dynamic "causal" relationship between the time series of nodal pairs, and is equivalent to Granger Causality, a form of directed functional connectivity (dFC)(Bressler & Seth, 2011; Silverstein et al., 2016). All modeling was performed using specifically written scripts (*R* software suite). Separate MVAR models were estimated from the fMRI BOLD time series of the ROIs for the Task Condition (Periodic and Pseudo-random) from each response hand (Right and Left). The MVAR model order indicating the number of previous time points in the model used to estimate a current time point, was one (Tang et al. 2012). Higher model orders were not tested because model order one was sufficient for meeting the aims of the study, and the interpretation of between-condition results from higher models would not capture network interactions at time scales that are proximate to the cognitive neurodynamics (that are observed at shorter time scales, typically in the millisecond range (K. D. Singh, 2012). A sliding window approach to MVAR modeling was adapted within each condition: first, task blocks from each condition were concatenated; then, separate MVAR models were estimated for each pair of time points, avoiding block boundaries; finally, the dFC values from each time point pair were averaged to yield the final dFC value.

For each nodal pair evaluated (21 pairs 7 nodes excluding the on-diagonal elements; two directions for each pair) eight MVAR coefficients were estimated for each participant: One for each Task Condition (Periodic or Pseudo-random), one for each Hand (Right or Left), and one for each direction of the pair (A → B or B → A). Then, these coefficients were forwarded to repeated measures analyses of variance performed on each pair. Each ANOVA had three factors (all modeled as within-subject's factors): Direction (A → B vs. B → A), Hand (Right vs. Left) and Condition (Random vs. Periodic). This approach provided a flexible assessment of the main effects of interest as well as higher order interactions.

Results

We organize the presentation of results as follows: 1) First, we present the results of the activation analyses, depicting activation conjunctions in our theoretically and experimentally motivated regions of interest (see Introduction). Using this data, we identified the nodes of interest forwarded for network analyses using uFC; 2) We then provide evidence of how the network of interest was modulated under each combination of the factors of response hand and task condition; 3) Next, we present results directly contrasting the factored conditions; 4) Lastly, we demonstrate the results of dFC analyses, to provide evidence of effects associated with Direction, Task Condition, Hand and potential interactions between them.

1. Activation Analysis

Figure 1 depicts identified clusters localized in areas consistent with other studies of finger movement responses with external sensory stimuli (Witt et al., 2008). Activation peaks in the left hemisphere, are consistent with previous studies involving simple motor tasks (Alahmadi et al., 2015; L. N. Singh et al., 1998). The extensive overlaps observed across the ROIs displayed in the BOLD activation map (Figure 1) highlight the value of deriving more specific and differentiable network interactions driving these activations (Friston, 2011).

2. Modulation of uFC as a function of Condition

uFC was used to identify pathways, the connectivity of which was significantly modulated by task, and then to investigate condition related differences in connectivity between co-activated nodes across the network. As seen in Figure 2, each combination of response hand and condition resulted in significant (relative to the null hypothesis) modulation of uFC (the figure shows patterns of increased and decreased uFC). The modulatory effects of task were largely positive, with only selective pathways characterized by a decrease in uFC. The significance effects in Figure 2 are presented in the form of binarized symmetric connectivity matrices in Figure 3. Significant modulation of pathways was most widely observed when the dominant right hand was used during the Periodic condition, that is, when a consistent motor set was established (Figure 3, top right).

Eight pathways were commonly modulated regardless of experimental condition (see Figures 2 and 3), and these effects suggest that these formed a common functional substrate underlying the task. When collapsed across Response Hand, the Periodic condition modulated connectivity of the following sub-networks Parietal Thalamus, Thalamus ⟷ PMC, PMC ⟷ M1, PMC ⟷ BG, BG ⟷ M1, and BG ⟷ Insula.

By comparison, only four pathways were significantly modulated regardless of response hand during the random condition, all associated with the basal ganglia: BG ⟷ M1, BG ⟷ Parietal, PMC ⟷ BG, and BG ⟷ Insula), with the Random condition inducing anti-correlations for M1 ⟷ Thalamus and Insula ⟷ Thalamus.

3. Comparison of uFC Based on Condition

Condition-related differences within Respond Hand: Figure 4 depicts Task condition related differences within each hand. The top panels depict connectivity matrices, color- coded by the *t*-statistic (see color bar) representing the change in uFC under periodic (warm colors) or random (cool colors) conditions. The connectomic rings in the bottom panel, represent the sub-networks wherein *significant* differences in uFC were observed to be greater either during periodic (warm colors) or random (cool colors) conditions (see color bar). As shown, condition specific differences were only observed for the right hand.

Comparison of Periodic and Random task conditions revealed that the Periodic condition induced greater uFC induced on the M1 ⟷ Thalamus pathway ($\beta = 0.57$, $t_{(19)} = 3.88$), and the SMA ⟷ Parietal pathway ($\beta = 0.30$, $t_{(19)} = 2.59$).

Response Hand-related differences within Condition: Figure 5 maintains the conventions used in Figure 4, but outlines hand-related effects *within* each condition.

When assessing for significance, hand-related differences were confined to the random condition wherein responding with the non-dominant left hand resulted in stronger modulation of pathway connectivity (connectomic ring, bottom left).

These effects were observed for the M1 ⟷ Thalamus ($\beta = 0.69$, $t_{(19)} = 4.26$), the PMC ⟷ Insula ($\beta = 0.23$, $t_{(19)} = 2.73$), SMA ⟷ Parietal ($\beta = 0.35$, $t_{(19)} = 2.30$) and BG ⟷ Thalamus ($\beta = 0.32$, $t_{(19)} = 2.16$) pathways.

4. Directed Functional Connectivity Analysis

The *un-thresholded* F- and p-matrices (Figure 6a and 6b) depict statistical effects associated with the Main Effect of Direction (A → B vs. B → A) for each analyses of variance conducted on sub-network pairs. Because the colors encode directional effects, these are *asymmetric* adjacency matrices. The vertical and horizontal axes are labeled “A” and “B” respectively: The warm colors indicate greater significance in the A → B direction, the cool colors indicate greater significance in the B → A direction (see color bar).

As seen, four significant main effects of Direction were observed (clearly indicated in the relevant cells), with two of these centering on the thalamus as target. MVAR coefficients for the BG → Thalamus ($F_{1,18}$=4.98, p<.039, *MSe*=.199) and SMA → Thalamus ($F_{1,18}$=6.98, *p*<.017, *MSe*=.201) were significantly greater than the opposite direction. In addition, the MVAR coefficient from the BG → Insula was significantly greater than the opposite direction ($F_{1,18}$=4.96, p<.039, *MSe*=.198), and the coefficient from the SMA → M1 was greater than the opposite direction ($_{FI,I8}$=11.34, p<.003, *MSe*=.093).

Other significant or marginally significant effects were observed. A main effect of Hand (Right ≠ Left) was observed for the SMA ⟷ Parietal pathway, ($F_{1,18}$=3.608, p<.05 one-tailed, *MSe*=.103), with the dFC on this pathway being greater when responding with the Left than the Right hand (See Figure 7a).

A significant interaction between Hand and Direction was observed on the M1 ⟷Thalamus pathway, ($F_{1,18}$=11–95, p<.003, *MSe*=.066). As seen in Figure 7b, M1 → Thalamus connectivity was greater for Left Hand responses, but Thalamus → M1 connectivity was greater for Right Hand responses. For this pathway, we also observed a marginally significant interaction between Direction and Condition, ($F_{1,18}$=3.389, p<.05 one-tailed, *MSe*=.087), largely driven by strong dFC for M1 → Thal during the Random condition (Figure 7c).

On the BG ⟷ Thalamus pathway, we observed a significant effect of Condition ($F_{1,18}$=7.358, *p*<.014, *MSe*=.046), with greater dFC observed during the Periodic, relative to the Random condition (Figure 7d).

Finally, on the Insula SMA pathway, we observed a marginally significant effect of Hand ($_{FI,I8}$=3.721, p<.05 one-tailed, MSe=.055), with greater dFC for the Right hand (Figure 7e).

Discussion

We used a basic visuo-motor integration paradigm with varying demands, to discover how task variations and/or response hand modulated the functional connectivity between regions in core and extended motor networks. The task differentially modulated uFC in an *a priori* suite of seven brain regions: pre-motor cortex, BG, insula, parietal lobe, SMA, M1, and thalamus. Each of the experimental conditions (created by a factorial combination of response hand and task condition), exerted unique (to the condition) and overlapping (with other conditions) effects on uFC (Figure 2). Our significant results were these: a) Eight pathways were consistently modulated across all conditions, with the SMA and the Parietal cortex figuring prominently: These pathways were SMA ⟷ BG, SMA ⟷ insula, SMA PMC, thalamus ⟷ BG, insula ⟷ PMC, parietal ⟷ SMA, parietal insula, and parietal ⟷ PMC. That the uFC of these sub-networks was modulated regardless of condition, suggests central roles for the SMA and the parietal cortex during the task that may relate to the initiation of finger movement and interactions between (Nachev, Kennard, & Husain, 2008; Pool et al., 2017; Tanji, 1994); b) More sub-networks were modulated when responding with the dominant right hand (Figure 3), suggesting a strong expression of hand dominance on observed functional patterns (Amunts et al., 1996); c) Significant task-related differences (Random ≠ Periodic) were confined to responses using the dominant right hand (Figure 4). This specificity for hand indicates pronounced expression of the dominant hand during conditions that promoted the use of a motor set and the synchronization of the movement (Witt et al., 2008). These effects are broadly consistent with previous independent studies using a similar paradigm (Asemi et al., 2015), and suggest that the induction of a motor set unfolds inherent representations of the dominant right hand through increased synchrony between key sub-networks. Moreover, these sub-networks include regions such as the thalamus and the parietal cortex that are committed to attention processing (Corbetta et al., 1998; Jagtap & Diwadkar, 2016), and the primary motor cortex (M1) and SMA wherein hand dominance is strongly expressed (Bernard & Seidler, 2012); d) In investigating hand-related differences within each task condition, the random condition induced the greatest modulation (Figure 5), specifically when responding with the non-dominant left hand. These effects are intriguing for multiple reasons: First, as previously noted the unpredictability of onsets during the random condition is challenging enough to preempt the establishment of a motor set during task epochs (Asemi et al., 2015) resulting in reactive responding. Second, in right handed participants, representations of the non-dominant left hand are distributed bi-laterally, unlike the contra-lateral mapping of the right hand to the left hemisphere (Diwadkar, Bellani, et al., 2017) which is relatively dominant for skilled or high fidelity motor movements (Haaland, Elsinger, Mayer, Durgerian, & Rao, 2004; Haaland, Harrington, & Knight, 2000; Volkmann et al., 1998). Consequently, the uFC of networks will be more strongly modulated under more stringent or reactive task conditions when participants respond with the “weaker” effector. Unsurprisingly, uFC on connections with “higher level” heteromodal centers associated with excitatory and inhibitory effects, including the PMC and the parietal cortex (Kolodny, Mevorach, & Shalev, 2017; Miller & Cohen, 2001) were more strongly modulated when the non-dominant left hand was used.

To compliment the uFC analyses, MVAR models were employed to observe directional effects among the regions. These analyses are consistent with principles in Granger Causality, and provided pair-wise assessment of effects between pairs. The results from these analyses show that significant effects of direction were observed and each of the experimental conditions (hand used and periodicity of stimuli) exerted specific effects on dFC (Figures 6 and 7). Our significant results were as follows: a) during the unimanual visuo-motor integration task four significant directional effects were observed including BG → Thalamus, SMA → Thalamus, BG → Insula, and SMA → M1 (Figure 6). These results suggest a central role of motor network regions exerting directional effects upon the thalamus consistent with thalamo-motor circuits previously described (Ahissar & Oram, 2013). Furthermore, SMA significantly exerted effects over both thalamus and M1 indicating that SMA has a predominant role in driving the networks related to finger movement in response to a visual stimulus (Guo, Schmitz, Mur, Ferreira, & Anderson, 2017); b) response hand exerted significant effects on dFC, with the SMA ←→Parietal pathway showing greater dFC for non-dominant left hand responses, but the Insula ←→ SMA pathway showing greater dFC for the dominant right hand (Figures 7a and 7e respectively). Generally, these effects track those from the uFC analyses, which showed that when using the non-dominant hand, brain regions such as the parietal cortex that are involved with attention processing are more active; c) When using the non-dominant hand, the M1 → Thalamus pathway showed great dFC, but in contrast when the dominant hand was used, the Thalamus → M1 connectivity was greater (Figure 7b). These effects provide evidence of differences in causal connectivity in the thalamus and primary motor cortex loop depending on hand used (dominant vs. non-dominant). The results are consistent with the uFC analyses, which indicated that the thalamus was involved in the development of a motor set and thus is capable of exerting effects back on M1 when the dominant hand is used, however the effect is reversed with the non-dominant hand suggesting that a motor-set starting from the thalamus may not be in place (Gao, Duan, Chen, 2011); d) The BG ←→Thalamus pathway had greater dFC during the Periodic condition relative to the Random condition (Figure 7d). These effects also generally track the uFC results showing that BG and thalamus circuits are involved in task conditions more amenable to developing a motor set; e) Finally, for the Random condition M1 → Thalamus dFC was strongest (Figure 7c). These results are similar to the results of the effects of hand used on dFC. In either situation, in the variable more likely to develop synchronicity (periodic condition or dominant hand), the thalamus exerted significant effects on the primary motor cortex. Whereas the opposite was true with the variables more likely to require higher cortical processing (random condition or non-dominant hand) where M1 exerted significant greater dFC on the thalamus. These results suggest that the M1 ←→ Thalamus sub-network's directional interactions are modified depending on complexity of task.

Task-driven changes are the strongest and most meaningful modulators of fMRI estimated functional profiles, which are driven by a combination of relatively slowly unfolding metabolic and vascular effects (Hoge et al., 1999; Logothetis, 2008). In addition to general task dynamics, fMRI signals are known to reflect representations of sensori-motor organization; Two classic examples are the retinotopic mapping of the visual fields to the ipsi- and contra-lateral visual cortex (Tootell, Mendola, Hadjikhani, Liu, & Dale, 1998), and

the center-surround organization of the visual cortex that can drive positive and negative BOLD responses (Shmuel, Augath, Oeltermann, & Logothetis, 2006). However, both activation and connectivity profiles induced within the same study and/or condition may reflect an admixture of *representation-based* and *task- based* processing. It is precisely this degree of flexibility in how the brain works and responds to/implements function that renders it challenging to understand structure- function-behavior relationships in the brain (Park & Friston, 2013). Distributed domain representations in the neural substrate can lead to unpredictable synchronies between functional networks, and these synchronies do not necessarily map in predictable ways to cognitive architectures (Price & Friston, 2005). Furthermore, higher-level cognitive architectures are themselves subjected to a multiplicity of feed-forward and feed-back interactions between uni-modal and heteromodal cortices (Mesulam, 1998); these interactions are unfolding at multiple time scales (Bressler & Tognoli, 2006; K. D. Singh, 2012). In this context, relatively circumscribed visuo-motor paradigms are well-suited, for tractably understanding task-dependent contextual modulation of the brain's functional pathways (Passingham, Stephan, & Kotter, 2002). This latter aspect motivated our study goals, and the combination of response hand and experimentally manipulated task conditions allowed us to discover their impact on sub-network uFC (Figures 2 & 3).

The juxtaposition of Figures 4 and 5 provide a useful illustration of how the uFC of the M1 ⟷ Thalamus and SMA ⟷ Parietal pathways are differentially modulated under combinations of effector use and condition. M1 is generally associated with effector representation, and is consistently activated during the initiation of finger movements (van den Berg, Swinnen, & Wenderoth, 2011), but its responses are also mediated by the cognitive characteristics of the task, evidence of a degree of flexibility in its functions in a range of cognitive paradigms (Tomasino & Gremese, 2016). The thalamus in addition to its role as an attention relay (Saalmann & Kastner, 2011), helps regulate and coordinate activity across motor regions (Ahissar & Oram, 2013), suggesting that the M1 ⟷ thalamus sub-network is an important motor-attention functional loop. Both the SMA and the parietal cortex have been implicated in command-related signaling of basic hand movements (Rathelot, Dum, & Strick, 2017), and their responses (Sale et al., 2017) and inter-regional interactions are known to underpin motor learning. As Figure 4 and Figure X demonstrates, the combination of responding with the dominant effector while establishing a motor set (periodic condition) induces greater uFC and dFC in these sub-networks, implying that the condition evokes representations of handedness. As Figure 5 and Figure X demonstrates, responding with the non-dominant effector during reactive response conditions induces greater undirected and directed functional connectivity, implying a greater representation of response difficulty when responding with the non-dominant hand.

Three additional pathways, SMA ⟷ PMC, BG ⟷ thalamus, and PMC ⟷ insula also showed greater representations of *reactive* responding when responding with the non-dominant effector (left hand). These effects in part must be presumed to reflect the complexity of responding with the non-dominant hand during uni-manual motor tasks (Sisti et al., 2011), and the increased synchrony between sub-networks thus sub serves execution of task complexity (Friedman et al., 2017). The representation of the basal ganglia, PMC and

the SMA in this effect is revealing given these region's roles in executive processing and motor control. Meta-analytic evidence has highlighted their roles in motor responding during stop/signal and go/no-go tasks, both paradigms which are characterized by reactive responding under uncertain stimulus onsets, similar to our study (Guo, Schmitz, Mur, Ferreira, & Anderson, 2017). Moreover, the synchrony between the SMA and primary cortex is associated with finger movements that underpin complex rhythmic patterns (Adhikari, Epstein, & Dhamala, 2017). Finally, meta analyses also implicate the thalamus as crucial for executive control mechanisms related to motor responding (Ardila, Bernal, & Rosselli, 2017), and all of these regions in mediating motor responses to conditional stimuli (Zapparoli, Seghezzi, & Paulesu, 2017).

Our study aims while modest underline the complexity of network dynamics even in the simplest of tasks and domains (Park & Friston, 2013). The modulation of functional connectivity in the brain's sub networks can reflect aspects of hand organization and/or how task complexity impacts motor function under different effector responses. In addition to reiterating apparent characteristics of brain function and organization, our results have implications for studying the pathophysiology of neurological and/or neuropsychiatric conditions with fMRI and motor paradigms (Abboud et al., 2017). Several of these conditions are characterized by motor deficits, yet have not been systematically studied using tractably administered tasks. Our effects suggest that it may be plausible to target motor network deficits in the brain using a combination of focused experimentation and connectivity analyses. Emerging studies using network analytic methods are beginning to document these effects even in disorders such as obsessive compulsive disorder (Friedman et al., 2017) hitherto not associated with motor dysfunction. Our ongoing work is focused both on using these methods to study aspects of motor organization and demand *and* evaluate brain network dysfunction in neuropsychiatric conditions.

Acknowledgements

Preparation of this work was supported by a Career Development Chair from Wayne State University, the Charles H. Gershenson Distinguished Faculty Fellowship from Wayne State University, the Lyckaki-Young Fund from the State of Michigan, the Prechter Family Bipolar Foundation, the Children's Hospital of Michigan Foundation, the Children's Research Center of Michigan, the Cohen Neuroscience Endowment, a Medical Student Internship from the Detroit Medical Center, and the National Institute of Mental Health (MH 59299).

REFERENCES

Abboud R, Noronha C, & Diwadkar VA (2017). Motor system dysfunction in the schizophrenia diathesis: Neural systems to neurotransmitters. Eur Psychiatry, 44, 125–133. [PubMed: 28641214]

Adhikari BM, Epstein CM, & Dhamala M (2017). Enhanced brain network activity in complex movement rhythms: a simultaneous fMRI-EEG study. Brain Connect.

Ahissar E, & Oram T (2013). Thalamic Relay or Cortico-Thalamic Processing? Old Question, New Answers. Cereb Cortex.

Alahmadi AA, Pardini M, Samson RS, D'Angelo E, Friston KJ, Toosy AT, et al. (2015). Differential involvement of cortical and cerebellar areas using dominant and nondominant hands: An FMRI study. Hum Brain Mapp, 36(12), 5079–5100. [PubMed: 26415818]

Amunts K, Schlaug G, Schleicher A, Steinmetz H, Dabringhaus A, Roland PE, et al. (1996). Asymmetry in the human motor cortex and handedness. Neuroimage, 4(3 Pt 1), 216–222. [PubMed: 9345512]

Ardila A, Bernal B, & Rosselli M (2017). Executive Functions Brain System: An Activation Likelihood Estimation Meta-analytic Study. Arch Clin Neuropsychol, 1–27. [PubMed: 28122764]

Asemi A, Ramaseshan K, Burgess A, Diwadkar VA, & Bressler SL (2015). Dorsal anterior cingulate cortex modulates supplementary motor area in coordinated unimanual motor behavior. Front Hum Neurosci, 9, 309. [PubMed: 26089783]

Bernard JA, & Seidler RD (2012). Hand dominance and age have interactive effects on motor cortical representations. PLoS ONE, 7(9), e45443. [PubMed: 23049800]

Bressler SL, & Seth AK (2011). Wiener-Granger causality: a well established methodology. Neuroimage, 58(2), 323–329. [PubMed: 20202481]

Bressler SL, Tang W, Sylvester CM, Shulman GL, & Corbetta M (2008). Top- down control of human visual cortex by frontal and parietal cortex in anticipatory visual spatial attention. J Neurosci, 28(40), 10056–10061. [PubMed: 18829963]

Bressler SL, & Tognoli E (2006). Operational principles of neurocognitive networks. Int J Psychophysiol, 60(2), 139–148. [PubMed: 16490271]

Buchanan RW, & Heinrichs DW (1989). The Neurological Evaluation Scale (NES): A structured instrument for the assessment of neurological signs in schizophrenia. Psychiatry Research, 27, 335–350. [PubMed: 2710870]

Corbetta M, Akbudak E, Conturo TE, Snyder AZ, Ollinger JM, Drury HA, et al. (1998). A common network of functional areas for attention and eye movements. Neuron, 21(4), 761–773. [PubMed: 9808463]

Cunnington R, Windischberger C, Deecke L, & Moser E (2003). The preparation and readiness for voluntary movement: a high-field event-related fMRI study of the Bereitschafts-BOLD response. Neuroimage, 20(1), 404–412. [PubMed: 14527600]

Diwadkar VA, Asemi A, Burgess A, Chowdury A, & Bressler SL (2017). Potentiation of motor sub-networks for motor control but not working memory: Interaction of dACC and SMA revealed by resting-state directed functional connectivity. PLoS One, 12(3), e0172531. [PubMed: 28278267]

Diwadkar VA, Bellani M, Chowdury A, Savazzi S, Perlini C, Marinelli V, et al. (2017). Activations in gray and white matter are modulated by uni-manual responses during within and inter-hemispheric transfer: effects of response hand and right-handedness. Brain Imaging Behav.

Diwadkar VA, Murphy ER, & Freedman RR (2014). Temporal Sequencing of Brain Activations During Naturally Occurring Thermoregulatory Events. Cereb Cortex, 24(3006–3013). [PubMed: 23787950]

Eickhoff SB, Bzdok D, Laird AR, Kurth F, & Fox PT (2012). Activation likelihood estimation meta-analysis revisited. Neuroimage, 59(3), 2349–2361. [PubMed: 21963913]

First MD, Gibbon M, Spitzer RL, Williams JBW, & Benjamin LS (1997). Structured clinical interview for DSM-IV Axis II personality disorders New York: Biometrics Research Department, NYSPI.

Fogassi L, Ferrari PF, Gesierich B, Rozzi S, Chersi F, & Rizzolatti G (2005). Parietal lobe: from action organization to intention understanding. Science, 308(5722), 662–667. [PubMed: 15860620]

Fogassi L, & Luppino G (2005). Motor functions of the parietal lobe. Curr Opin Neurobiol, 15(6), 626–631. [PubMed: 16271458]

Friedman A, Burgess A, Ramaseshan K, Easter P, Khatib D, Chowdury A, et al. (2017). Brain network dysfunction in obsessive-compulsive disorder induced by simple uni-manual behavior: The role of the dorsal anterior cingulate cortex. Psychiatry Res Neuroimaging, 260, 6–15. [PubMed: 27992792]

Friston KJ (2011). Functional and effective connectivity: a review. Brain Connect, 1(1), 13–36. [PubMed: 22432952]

Ghaziri J, Tucholka A, Girard G, Houde JC, Boucher O, Gilbert G, et al. (2017). The Corticocortical Structural Connectivity of the Human Insula. Cereb Cortex, 27(2), 1216–1228. [PubMed: 26683170]

Goble DJ, Coxon JP, Van Impe A, De Vos J, Wenderoth N, & Swinnen SP. The neural control of bimanual movements in the elderly: Brain regions exhibiting age-related increases in activity, frequency-induced neural modulation, and task-specific compensatory recruitment. Hum Brain Mapp, 31(8), 1281–1295.

Goense JB, & Logothetis NK (2008). Neurophysiology of the BOLD fMRI signal in awake monkeys. Curr Biol, 18(9), 631–640. [PubMed: 18439825]

Grafton ST, Hazeltine E, & Ivry RB (2002). Motor sequence learning with the nondominant left hand. A PET functional imaging study. Exp Brain Res, 146(3), 369–378. [PubMed: 12232693]

Grafton ST, Mazziotta JC, Woods RP, & Phelps ME (1992). Human functional anatomy of visually guided finger movements. Brain, 115 (Pt 2), 565–587. [PubMed: 1606482]

Grefkes C, Eickhoff SB, Nowak DA, Dafotakis M, & Fink GR (2008). Dynamic intra- and interhemispheric interactions during unilateral and bilateral hand movements assessed with fMRI and DCM. Neuroimage, 41(4), 1382–1394. [PubMed: 18486490]

Guo Y, Schmitz TW, Mur M, Ferreira CS, & Anderson MC (2017). A supramodal role of the basal ganglia in memory and motor inhibition: Meta- analytic evidence. Neuropsychologia, 108, 117–134. [PubMed: 29199109]

Guye M, Parker GJ, Symms M, Boulby P, Wheeler-Kingshott CA, Salek- Haddadi A, et al. (2003). Combined functional MRI and tractography to demonstrate the connectivity of the human primary motor cortex in vivo. Neuroimage, 19(4), 1349–1360. [PubMed: 12948693]

Haaland KY, Elsinger CL, Mayer AR, Durgerian S, & Rao SM (2004). Motor sequence complexity and performing hand produce differential patterns of hemispheric lateralization. J Cogn Neurosci, 16(4), 621–636. [PubMed: 15165352]

Haaland KY, Harrington DL, & Knight RT (2000). Neural representations of skilled movement. Brain, 123 (Pt 11), 2306–2313. [PubMed: 11050030]

Hoffstaedter F, Grefkes C, Caspers S, Roski C, Palomero-Gallagher N, Laird AR, et al. (2014). The role of anterior midcingulate cortex in cognitive motor control: evidence from functional connectivity analyses. Hum Brain Mapp, 35(6), 2741–2753. [PubMed: 24115159]

Hoge RD, Atkinson J, Gill B, Crelier GR, Marrett S, & Pike GB (1999). Stimulus-dependent BOLD and perfusion dynamics in human V1. Neuroimage, 9(6 Pt 1) 573–585. [PubMed: 10334901]

Jagtap P, & Diwadkar VA (2016). Effective connectivity of ascending and descending frontalthalamic pathways during sustained attention: Complex brain network interactions in adolescence. Hum Brain Mapp, 37(7), 2557–2570. [PubMed: 27145923]

Kim SG, Ashe J, Hendrich K, Ellermann JM, Merkle H, Ugurbil K, et al. (1993). Functional magnetic resonance imaging of motor cortex: hemispheric asymmetry and handedness. Science, 261(5121), 615–617. [PubMed: 8342027]

Kolodny T, Mevorach C, & Shalev L (2017). Isolating response inhibition in the brain: Parietal versus frontal contribution. Cortex, 88, 173–185. [PubMed: 28142026]

Lehericy S, Bardinet E, Tremblay L, Van de Moortele PF, Pochon JB, Dormont D, et al. (2006). Motor control in basal ganglia circuits using fMRI and brain atlas approaches. Cereb Cortex, 16(2), 149–161. [PubMed: 15858164]

Logothetis NK (2008). What we can do and what we cannot do with fMRI. Nature, 453(7197), 869–878. [PubMed: 18548064]

Lotze M, Erb M, Flor H, Huelsmann E, Godde B, & Grodd W (2000). fMRI evaluation of somatotopic representation in human primary motor cortex. Neuroimage, 11(5 Pt 1), 473–481. [PubMed: 10806033]

Maldjian JA, Laurienti PJ, Kraft RA, & Burdette JH (2003). An automated method for neuroanatomic and cytoarchitectonic atlas-based interrogation of fMRI data sets. Neuroimage, 19(3), 1233–1239. [PubMed: 12880848]

Mesulam MM (1998). From sensation to cognition. Brain, 121, 1013–1052. [PubMed: 9648540]

Miller EK, & Cohen JD (2001). An integrative theory of prefrontal cortex function. Annu Rev Neurosci, 24, 167–202. [PubMed: 11283309]

Muzik O, & Diwadkar VA (2016). In vivo correlates of thermoregulatory defense in humans: Temporal course of sub-cortical and cortical responses assessed with fMRI. Hum Brain Mapp, 37(9), 3188–3202. [PubMed: 27220041]

Nachev P, Kennard C, & Husain M (2008). Functional role of the supplementary and pre-supplementary motor areas. Nature Reviews Neuroscience, 9(11), 856–869. [PubMed: 18843271]

Nichols T, Brett M, Andersson J, Wager T, & Poline JB (2005). Valid conjunction inference with the minimum statistic. Neuroimage, 25(3), 653–660. [PubMed: 15808966]

Park HJ, & Friston K (2013). Structural and functional brain networks: from connections to cognition. Science, 342(6158), 1238411. [PubMed: 24179229]

Passingham RE, Stephan KE, & Kotter R (2002). The anatomical basis of functional localization in the cortex. Nat Rev Neurosci, 3(8), 606–616. [PubMed: 12154362]

Paus T (2001). Primate anterior cingulate cortex: where motor control, drive and cognition interface. Nat Rev Neurosci, 2(6), 417–424. [PubMed: 11389475]

Pool EM, Leimbach M, Binder E, Nettekoven C, Eickhoff SB, Fink GR, et al. (2017). Network dynamics engaged in the modulation of motor behavior in stroke patients. Hum Brain Mapp.

Pool EM, Rehme AK, Eickhoff SB, Fink GR, & Grefkes C (2015). Functional resting-state connectivity of the human motor network: differences between right- and left-handers. Neuroimage, 109, 298–306. [PubMed: 25613438]

Pool EM, Rehme AK, Fink GR, Eickhoff SB, & Grefkes C (2014). Handedness and effective connectivity of the motor system. Neuroimage, 99, 451–460. [PubMed: 24862079]

Price CJ, & Friston KJ (2005). Functional ontologies for cognition: The systematic definition of structure and function. Cogn Neuropsychol, 22(3), 262–275. [PubMed: 21038249]

Rathelot JA, Dum RP, & Strick PL (2017). Posterior parietal cortex contains a command apparatus for hand movements. Proc Natl Acad Sci U S A, 114(16), 4255–4260. [PubMed: 28373554]

Saalmann YB, & Kastner S (2011). Cognitive and perceptual functions of the visual thalamus. Neuron, 71(2), 209–223. [PubMed: 21791281]

Sale MV, Reid LB, Cocchi L, Pagnozzi AM, Rose SE, & Mattingley JB (2017). Brain changes following four weeks of unimanual motor training: Evidence from behavior, neural stimulation, cortical thickness, and functional MRI. Hum Brain Mapp, 38(9), 4773–4787. [PubMed: 28677224]

Sarfeld AS, Diekhoff S, Wang LE, Liuzzi G, Uludag K, Eickhoff SB, et al. (2012). Convergence of human brain mapping tools: neuronavigated TMS parameters and fMRI activity in the hand motor area. Hum Brain Mapp, 33(5), 1107–1123. [PubMed: 21520346]

Seizeur R, Magro E, Prima S, Wiest-Daessle N, Maumet C, & Morandi X (2014). Corticospinal tract asymmetry and handedness in right- and left-handers by diffusion tensor tractography. Surg Radiol Anat, 36(2), 111–124. [PubMed: 23807198]

Shmuel A, Augath M, Oeltermann A, & Logothetis NK (2006). Negative functional MRI response correlates with decreases in neuronal activity in monkey visual area V1. Nat Neurosci, 9(4), 569–577. [PubMed: 16547508]

Silverstein B, Bressler S, & Diwadkar VA (2016). Inferring the disconnection syndrome in schizophrenia: Interpretational considerations on methods for the network analyses of fMRI data. Front Psychiatry, 7, 132. [PubMed: 27536253]

Singh KD (2012). Which “neural activity” do you mean? fMRI, MEG, oscillations and neurotransmitters. Neuroimage, 62(2), 1121–1130. [PubMed: 22248578]

Singh LN, Higano S, Takahashi S, Kurihara N, Furuta S, Tamura H, et al. (1998). Comparison of ipsilateral activation between right and left handers: a functional mR imaging study. Neuroreport, 9(8), 1861–1866. [PubMed: 9665616]

Sisti HM, Geurts M, Clerckx R, Gooijers J, Coxon JP, Heitger MH, et al. . Testing multiple coordination constraints with a novel bimanual visuomotor task. PLoS One, 6(8), e23619.

Tang W, Bressler SL, Sylvester CM, Shulman GL, & Corbetta M (2012). Measuring Granger Causality between cortical regions from voxelwise fMRI BOLD signals with LASSO. PLoS Comput Biol, 8(5), e1002513. [PubMed: 22654651]

Tanji J (1994). The supplementary motor area in the cerebral cortex. Neurosci Res, 19(3), 251–268. [PubMed: 8058203]

Tomasino B, & Gremese M (2016). The Cognitive Side of M1. Front Hum Neurosci, 10, 298. [PubMed: 27378891]

Tootell RB, Mendola JD, Hadjikhani NK, Liu AK, & Dale AM (1998). The representation of the ipsilateral visual field in human cerebral cortex. Proc Natl Acad Sci U S A, 95(3), 818–824. [PubMed: 9448246]

Tzourio-Mazoyer N, Petit L, Zago L, Crivello F, Vinuesa N, Joliot M, et al. (2015). Between-hand difference in ipsilateral deactivation is associated with hand lateralization: fMRI mapping of 284 volunteers balanced for handedness. Front Hum Neurosci, 9, 5. [PubMed: 25705184]

Uddin LQ, Nomi JS, Hebert-Seropian B, Ghaziri J, & Boucher O (2017). Structure and Function of the Human Insula. J Clin Neurophysiol, 34(4), 300–306. [PubMed: 28644199]

van den Berg FE, Swinnen SP, & Wenderoth N (2011). Involvement of the primary motor cortex in controlling movements executed with the ipsilateral hand differs between left- and right-handers. J Cogn Neurosci, 23(11), 3456–3469. [PubMed: 21452954]

Velikova S, Locatelli M, Insacco C, Smeraldi E, Comi G, & Leocani L (2010). Dysfunctional brain circuitry in obsessive-compulsive disorder: source and coherence analysis of EEG rhythms. Neuroimage, 49(1), 977–983. [PubMed: 19683062]

Volkmann J, Schnitzler A, Witte OW, & Freund H (1998). Handedness and asymmetry of hand representation in human motor cortex. J Neurophysiol, 79(4), 2149–2154. [PubMed: 9535974]

Whitfield-Gabrieli S, & Nieto-Castanon A (2012). Conn: a functional connectivity toolbox for correlated and anticorrelated brain networks. Brain Connect, 2(3), 125–141. [PubMed: 22642651]

Witt ST, Laird AR, & Meyerand ME (2008). Functional neuroimaging correlates of finger-tapping task variations: an ALE meta-analysis. Neuroimage, 42(1), 343–356. [PubMed: 18511305]

Witt ST, & Stevens MC (2013). The role of top-down control in different phases of a sensorimotor timing task: a DCM study of adults and adolescents. Brain Imaging Behav, 7(3), 260–273. [PubMed: 23475755]

Zapparoli L, Seghezzi S, & Paulesu E (2017). The What, the When, and the Whether of Intentional Action in the Brain: A Meta-Analytical Review. Front Hum Neurosci, 11, 238. [PubMed: 28567010]

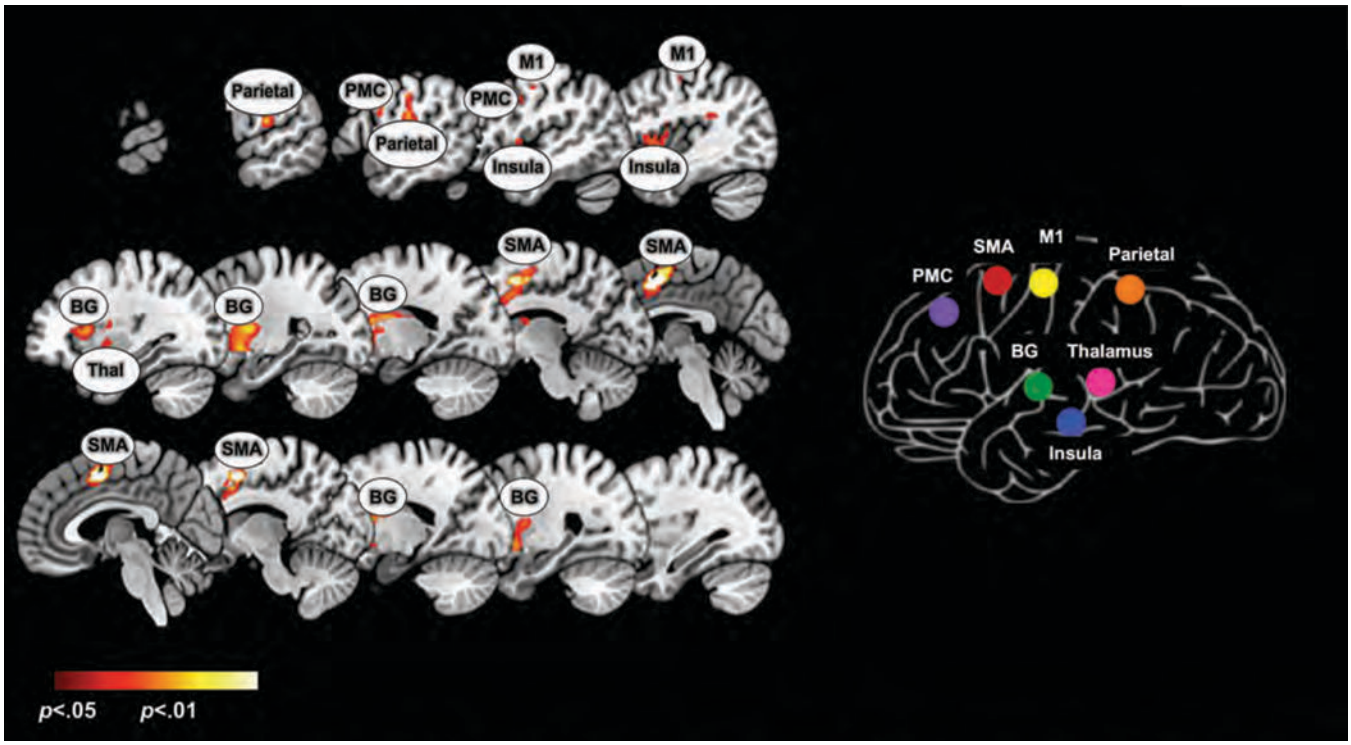

Figure 1.

The left panel depicts the results of a conjunction analysis (Left Hand ∩ Right Hand) derived from second level random effects model (see Methods). Significant clusters ($p<0.05$, cluster level) under this analysis depict regions co-activated regardless of the hand used in responding. Results are overlaid on a mosaic of sagittal slices with peaks in the BG, PMC, Insula, M1, SMA, parietal, and thalamus labelled. These peaks were forwarded for uFC analyses, and the figure on the right reveals the reduced matrix of regions (see also Figures 3–5). Subsequent figures/analyses are focused on quantifying changes in the uFC of sub-networks in this matrix.

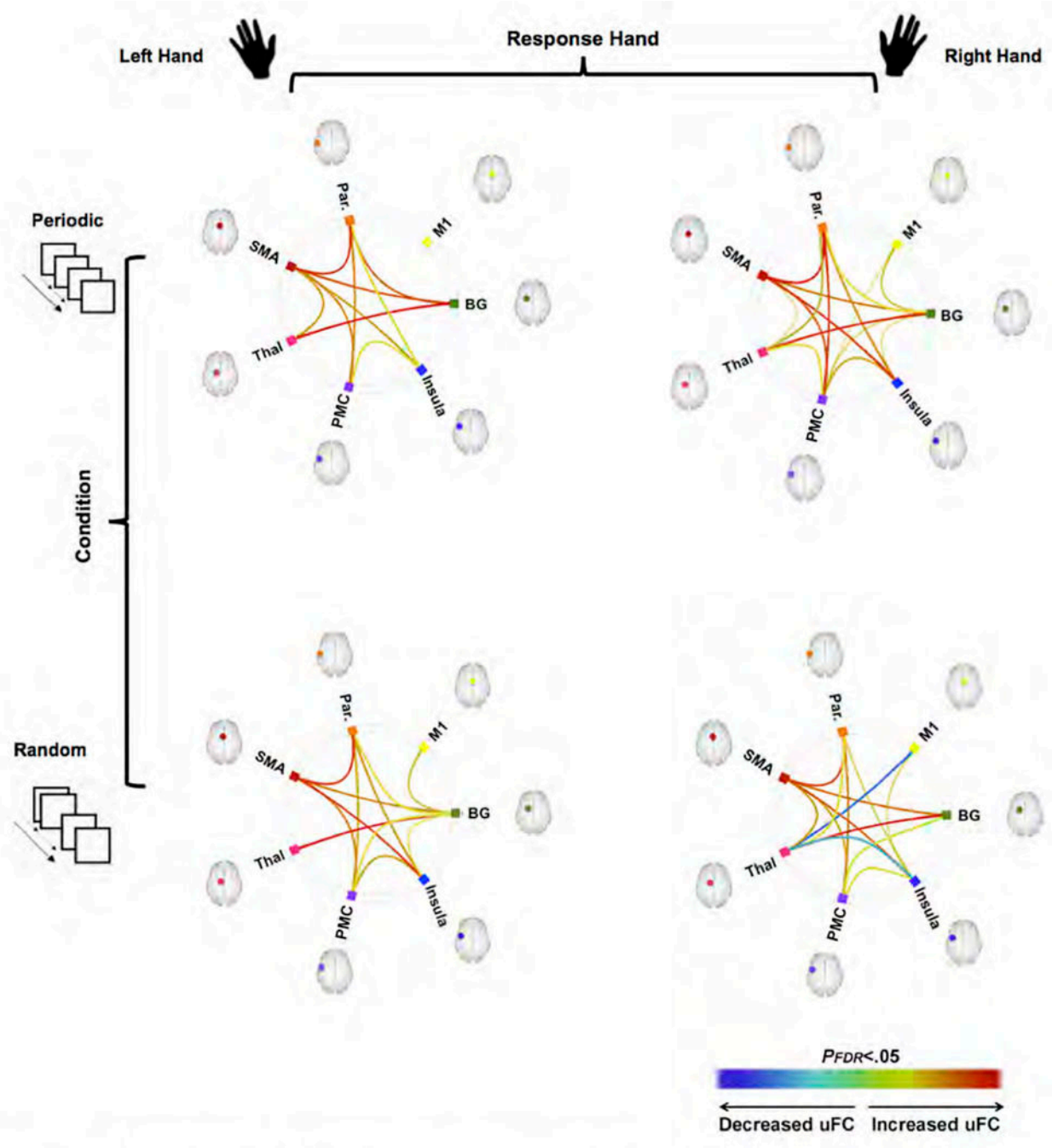

Figure 2.

The framework of the overall experimental design and analyses are depicted with each of the two factors, Response Hand (Left vs. Right) and Visuo-Motor Condition (Periodic vs. Random) shown horizontally and vertically respectively (for a total of four conditions). Under this framework and in each of the connectomic rings, we denote edges representing sub-networks the uFC between which was significantly modulated under each condition (warm colors represent increased uFC, cool colors represent decreased uFC).

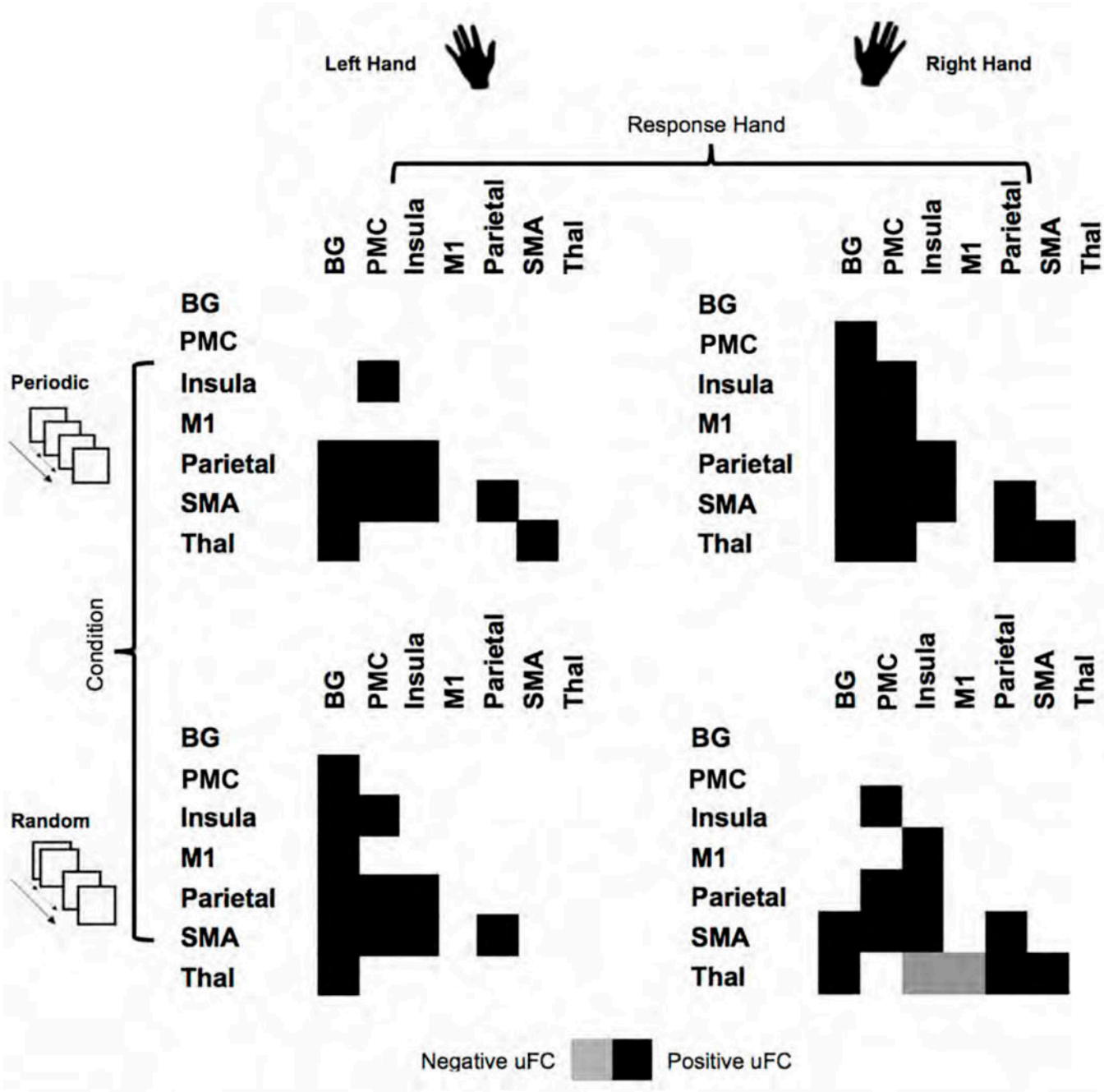

Figure 3.

The connectomic rings from Figure 2 are re-represented in (symmetric) adjacency matrices. As depicted here, each condition induces specific patterns of uFC (filled positive or negative matric locations). with the combination of dominant (right) hand and periodic condition inducing the highest degree of uFC modulation, and the combination of non-dominant (left) hand and periodic condition inducing the lowest degree of uFC.

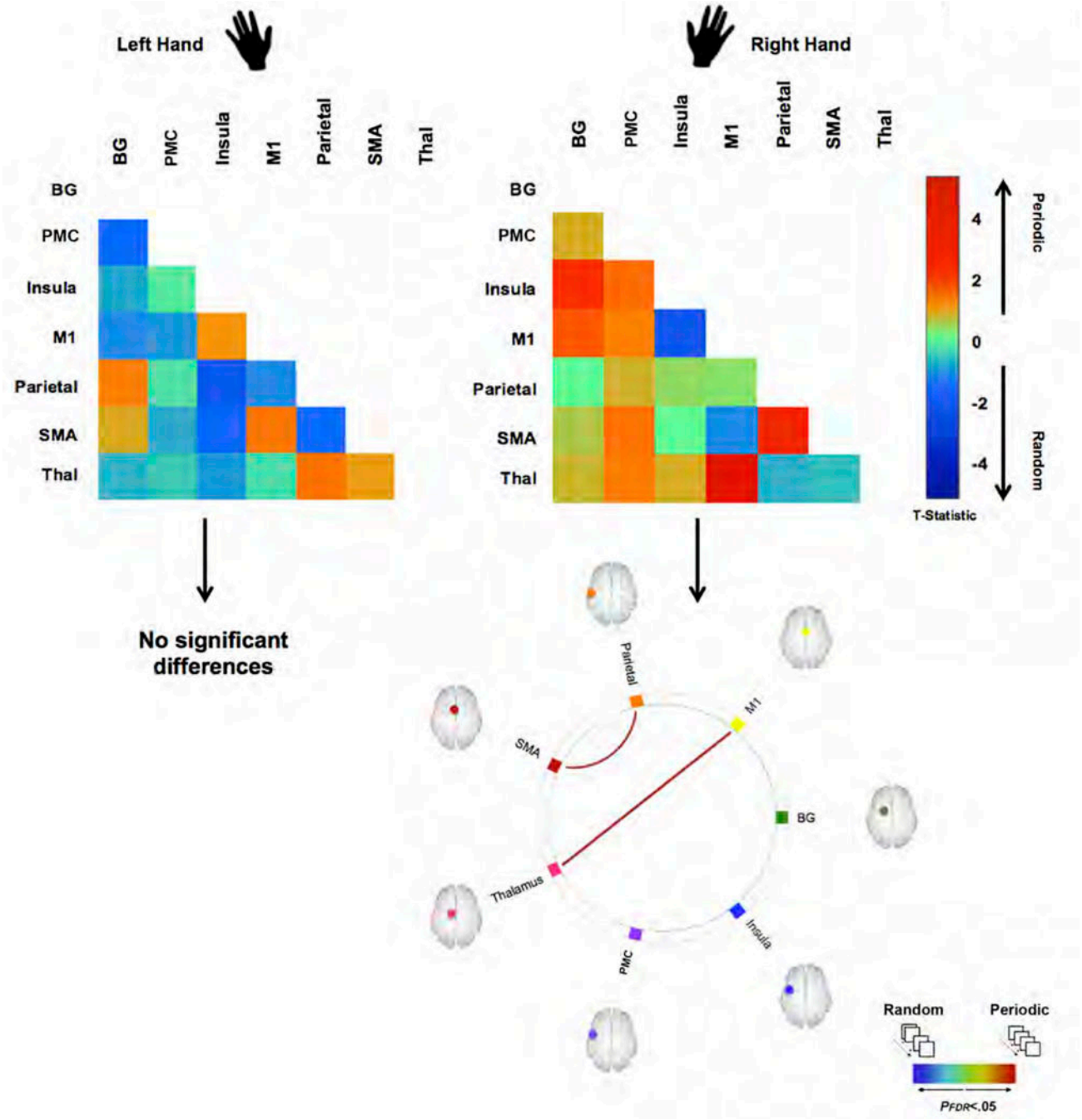

Figure 4.

The figure depicts how visuo-motor condition (Periodic vs. Random) induces differences in uFC under responding with the dominant Right hand or Left hand. The adjacency matrices depicted unthresholded *t*-maps. A positive t-statistic indicates greater uFC during the Periodic condition (warm colors) and a negative t-statistic indicates greater uFC during the Random condition (cool colors). Below these "heat" matrices, we present statistically thresholded differences, depicted as edges in the connectomic rings. As seen, only when responding with the dominant Right Hand do we observe differences in induced uFC

between the two conditions (Periodic > Random), observed on the M1⟷ thalamus and Parietal ⟷ SMA sub-networks.

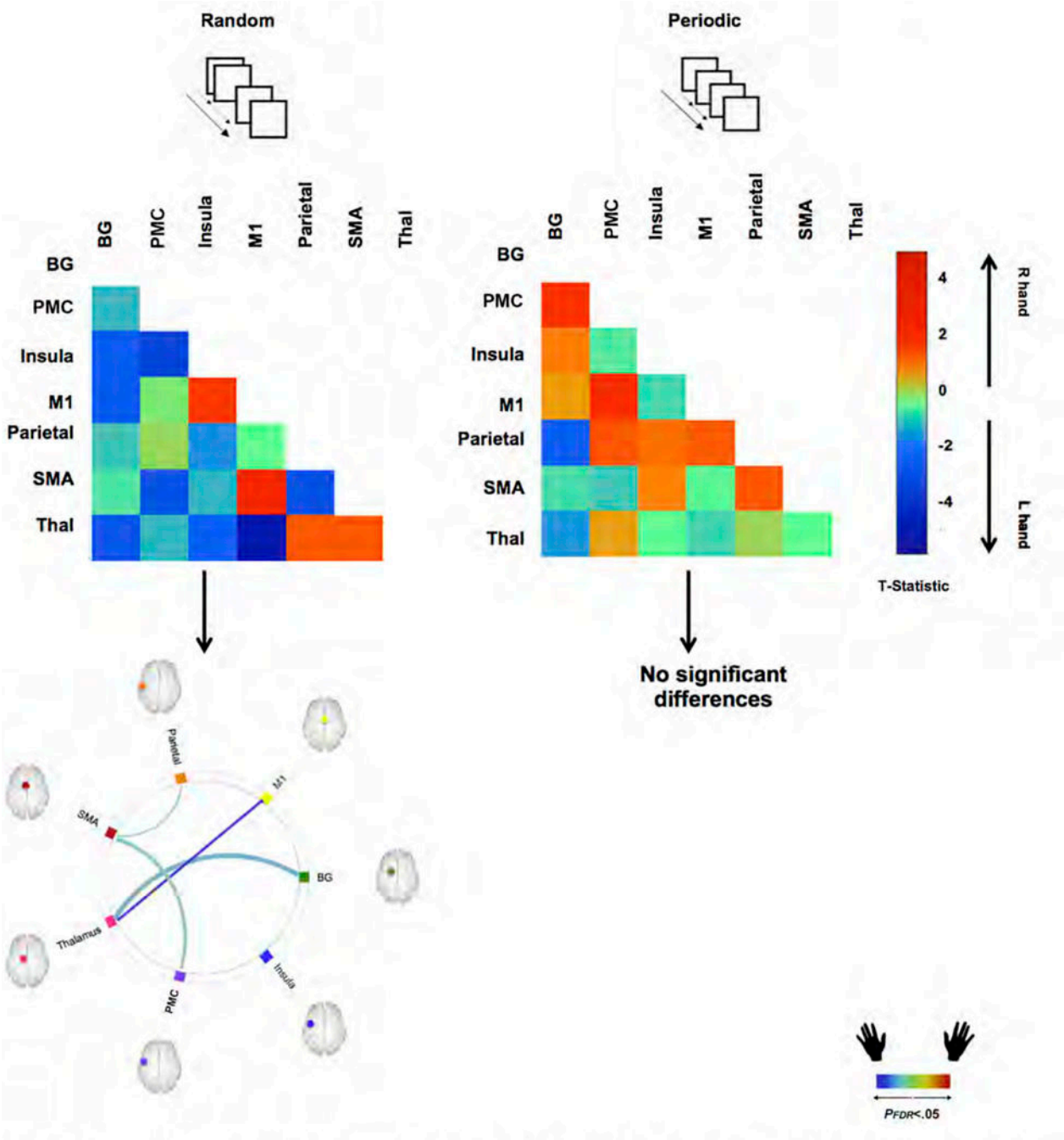

Figure 5.

The figure depicts how Response Hand (Right vs. Left) induces differences in uFC under each of the Periodic or Random visuo-motor conditions. The adjacency matrices depicted unthresholded t-maps. A positive *t*-statistic indicates greater uFC when responding with the Right Hand (warm colors) and a negative *t*-statistic indicates greater uFC when responding with the Left Hand (cool colors). Below these "heat" matrices, we present statistically thresholded differences, depicted as edges in the connectomic rings. As seen, significant

differences are only observed under the Random condition, wherein responding with the Left Hand induces greater uFC in multiple sub-networks (see text).

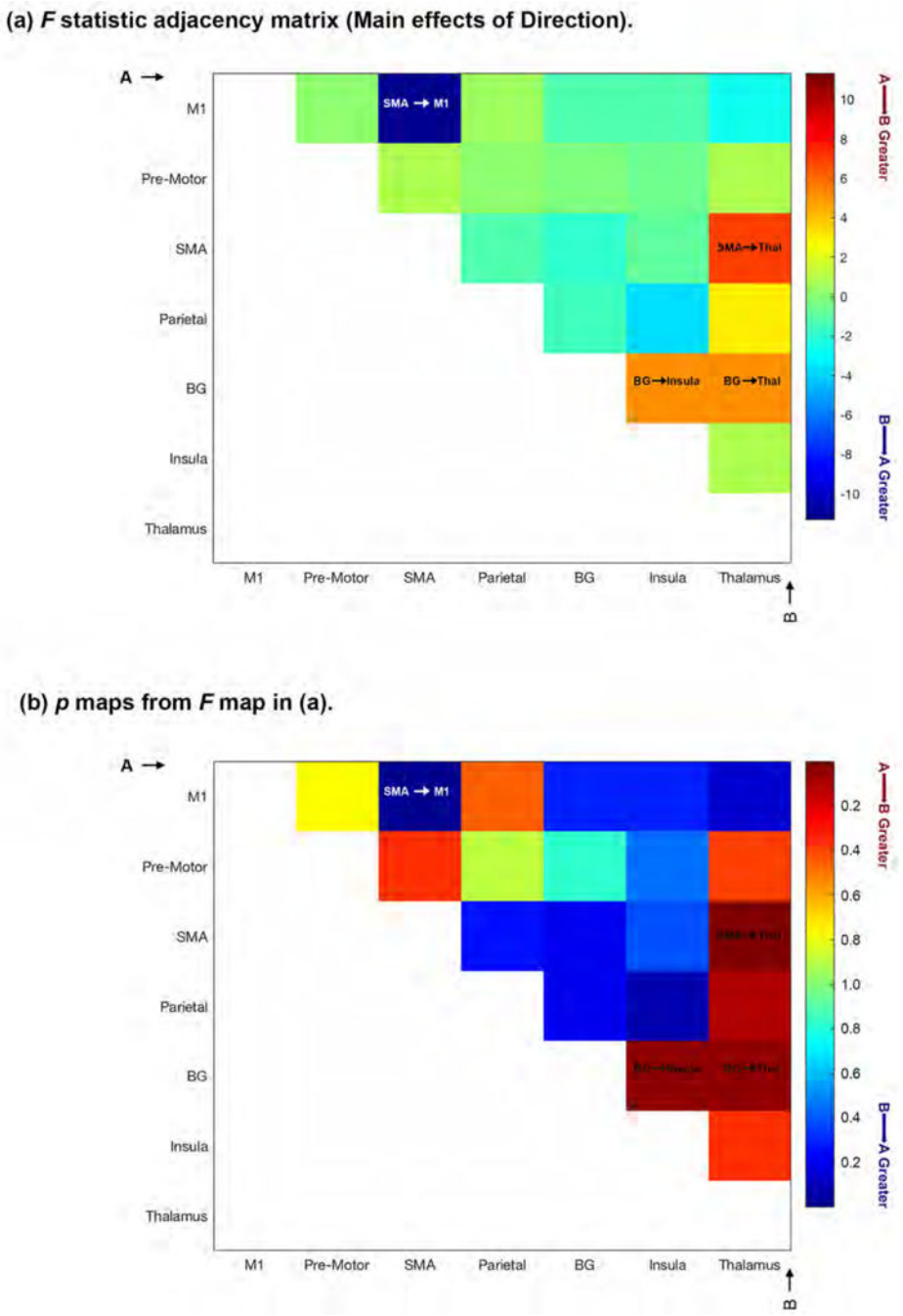

Figure 6.

The figure depicts *un-thresholded* F- (6a) and p-matrices (6b) depicting statistical effects associated with the Main Effect of Direction (A → B vs. B → A) for each analyses of variance conducted on sub-network pairs. The colors encode directional effects, resulting in *asymmetric* adjacency matrices. The vertical and horizontal axes are labeled "A" and "B" respectively: The warm colors indicate greater significance in the A → B direction, the cool colors indicate greater significance in the B → A direction (see color bar). Four significant main effects of Direction were observed (clearly indicated in the relevant cells): BG →

Thalamus, SMA → Thalamus, BG → Insula and SMA → M1 (see Results for detailed statistical information.

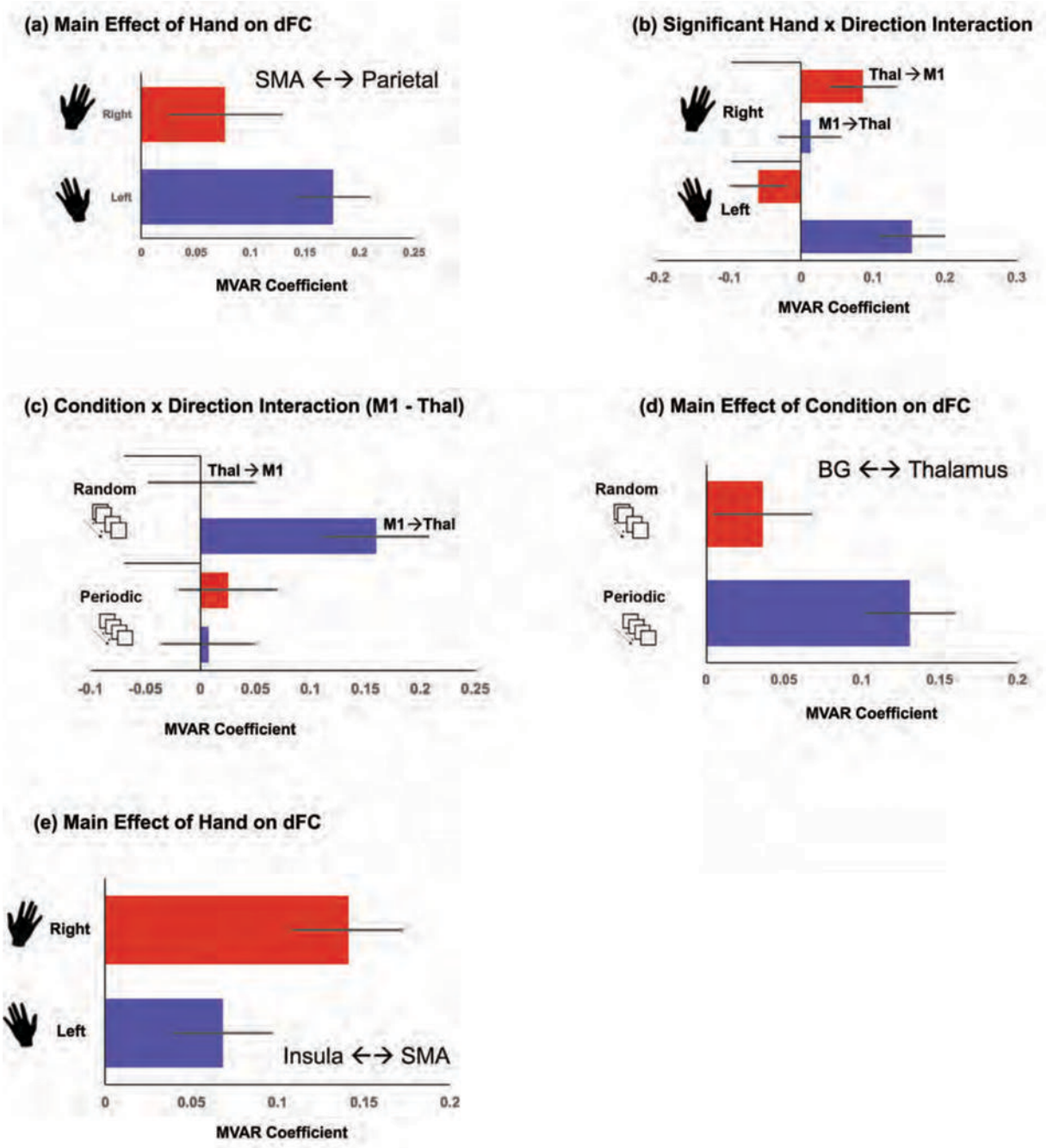

Figure 7.

The Figure depicts ancillary effects from the dFC analyses to show: a) greater dFC during Left hand, than Right hand responses on the SMA ⟷ Parietal pathway, b) a significant Hand x Direction interaction on the M1 ⟷ Thalamus pathway, c) A significant Condition x Direction interaction on the M1 ⟷ Thalamus pathway, d) greater dFC during Periodic compared to Random conditions on the BG ⟷ Thalamus pathway, and e) marginally greater dFC during Right hand, than Left hand responses on the Insula ⟷ SMA pathway.

In all graphs, we plot the estimated MVAR coefficient (see Methods), and error bars are ± sem.

Table 1.

The table provides statistical and spatial information for cluster extents (p<.05) and significance peaks (Figure 1) forwarded for uFC analyses (Figures 2–5).

ROI	MNI Coordinates			Cluster Extent Threshold (k)	Peak-level T-statistic
	X	Y	Z		
BG	−24	−1	9	191	4.51
PMC	−51	0	36	45	4.39
Insula	−46	2	3	175	3.76
M1	−46	−6	48	27	4.17
Parietal	−60	−16	21	229	4.46
SMA	−2	3	52	331	5.91
Thalamus	−15	−10	13	87	2.59